A p53 enhancer region regulates target genes through chromatin conformations in *cis* and in *trans*

Nichole Link, Paula Kurtz, Melissa O'Neal, Gianella Garcia-Hughes, and John M. Abrams[1]

Department of Cell Biology, University of Texas Southwestern Medical Center, Dallas, Texas 75390, USA

We examined how a p53 enhancer transmits regulatory information in vivo. Using genetic ablation together with digital chromosome conformation capture and fluorescent in situ hybridization, we found that a *Drosophila* p53 enhancer region (referred to as the p53 response element [p53RE]) physically contacts targets in *cis* and across the centromere to control stress-responsive transcription at these sites. Furthermore, when placed at ectopic genomic positions, fragments spanning this element re-established chromatin contacts and partially restored target gene regulation to mutants lacking the native p53RE. Therefore, a defined p53 enhancer region is sufficient for long-range chromatin interactions that enable multigenic regulation.

Supplemental material is available for this article.

Received June 30, 2013; revised version accepted October 10, 2013.

The p53 gene is mutated in a majority of human cancers (Vousden and Prives 2009; Freed-Pastor and Prives 2012). The product of this tumor suppressor regulates transcription of downstream target genes through response elements containing a defined DNA-binding site (for review, see Menendez et al. 2009), and most mutations found in cancer patients are thought to affect this activity (Vousden and Prives 2009). Features of the p53 network that regulate stress-responsive transcription are also evolutionarily conserved (Lu et al. 2009). Like its human counterpart, *Drosophila* p53 responds to genotoxic stress and integrates adaptive responses at the cellular level (Brodsky et al. 2000; Ollmann et al. 2000; Sogame et al. 2003). A well-characterized p53 response element (p53RE) located 4.8 kb upstream of the proapoptotic gene *reaper* (*rpr*) consists of adjacent 10mers virtually identical to the human p53-binding consensus sequence (Brodsky et al. 2000). This element is thought to function as a stress-responsive enhancer by recruiting p53 and inducing *rpr* (Brodsky et al. 2000). Genome-wide analyses identified additional DNA damage-responsive genes that also depend on p53 for induction (known as RIPD [radiation-induced p53-dependent] genes) (Akdemir et al. 2007), including two other genes in the Reaper region (*hid* and *sickle* [*skl*]) and others located throughout the genome (Brodsky et al. 2004; Akdemir et al. 2007). Presumably, other regulatory elements control these genes.

Here, we used the *Drosophila* model to genetically examine a single p53 enhancer in vivo. This p53 enhancer region conferred *cis* regulation on multiple genes spanning 330 kb in the Reaper region. Surprisingly, this same enhancer also controlled stimulus-responsive induction of unlinked target genes mapping across the centromere. Using digital chromosome conformation capture (d3C) together with fluorescent in situ hybridization (FISH), we found that the p53RE physically contacts local and long-distance target sites via looping interactions. Furthermore, when ectopically positioned to a nonnative chromosome, the p53 enhancer re-established long-range contacts and regulation to target genes in mutants lacking the native element. Together, these observations establish that p53 enhancer elements can specify genome-scale regulation through the assembly of chromatin interactions in *cis* and in *trans*.

Results and Discussion

A defined p53 enhancer region regulates multiple target genes in cis

To genetically examine the function of a canonical p53 enhancer, we eliminated a well-studied p53 enhancer region (the p53RE) that maps upstream of the *rpr* gene. The Exelixis transposon collection enabled rapid production of a genomic deletion that removes the p53RE ($D2^{p53RE}$) (Fig. 1) using FRT-mediated recombination (see the Supplemental Material). Another FRT deletion, $D3^{control}$, removes the neighboring sequence but leaves the p53RE intact and is used throughout our studies as a control. To examine whether animals lacking the p53RE were affected for p53-dependent, stress-induced cell death, we treated early embryos with ionizing irradiation and stained with acridine orange, a marker for apoptotic cells (Abrams et al. 1993). Robust induction of apoptosis is seen in control embryos but not in $p53^{-}$ animals (Sogame et al. 2003) or $D2^{p53RE}$ mutants (Figs. 1E,F, 4E [below]). To examine how activity from the p53 enhancer might be linked to defects seen in $D2^{p53RE}$ animals, we measured p53-dependent gene expression in staged $D2^{p53RE}$ and $D3^{control}$ embryos. As previously reported by others and us (Brodsky et al. 2004; Akdemir et al. 2007), *rpr*, *hid*, and *skl* are induced after radiation challenge in wild-type (w^{1118}) but not $p53^{-}$ embryos (Fig. 1B–D). Similarly, in $D2^{p53RE}$ mutants, *rpr* was completely nonresponsive (Fig. 1B), but regulation of this gene was unperturbed in $D3^{control}$ (Fig. 1B) and $D2^{p53RE}$ heterozygous animals (Supplemental Fig. 1A). Furthermore, p53 expression was unaffected in $D2^{p53RE}$ mutants (Supple-

[*Keywords*: genome architecture; chromosome conformation capture; p53; apoptosis; long-distance gene regulation]
[1]Corresponding author
E-mail john.abrams@utsouthwestern.edu
Article is online at http://www.genesdev.org/cgi/doi/10.1101/gad.225565.113.

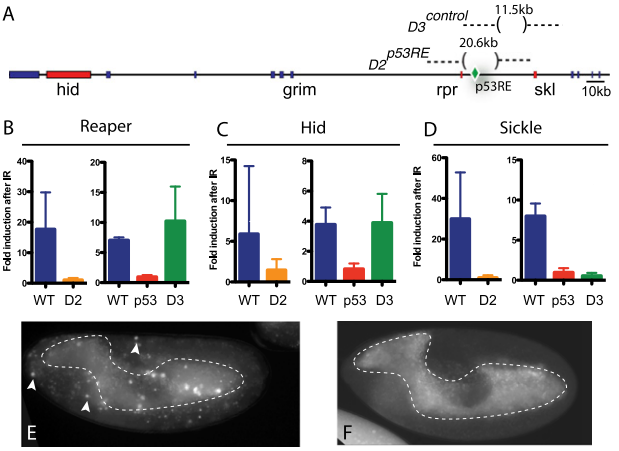

Figure 1. A p53 enhancer region controls stimulus-induced transcription of multiple genes in the Reaper region. (*A*) Annotated protein-coding genes in the Reaper region on 3L are labeled (from *Drosophila melanogaster* assembly release 5 coordinates 18,150,842–18,485,841). Proapoptotic genes are red, and others are blue. Tailored deletions are indicated (brackets), with interval size noted *above*. The p53-binding site (green diamond) is eliminated in the $D2^{p53RE}$ deletion but remains intact in the $D3^{control}$ deletion. (*B–D*) Radiation-induced expression of RIPD genes in the Reaper region. Quantitative RT–PCR was used to assess wild-type, $D2^{p53RE}$, $D3^{control}$, and *p53* mutant embryos, and fold induction is shown. Note that *rpr* (*B*), *hid* (*C*), and *skl* (*D*) are nonresponsive in $D2^{p53RE}$ animals but respond in $D3^{control}$ with the exception of *skl* (the $D3^{control}$ breakpoint is <2 kb from this gene). (*B–D*) $p53^{-}$ animals are unresponsive for all genes tested. Plots show the average of three biological replicates, with the standard deviation indicated. *rp49* expression was used for normalization. (*E*) Acridine orange staining of an early wild-type embryo after treatment with irradiation. The yolk is outlined, and arrows indicate examples of dying cells. (*F*) Acridine orange staining of a similarly aged $D2^{p53RE}$ embryo after treatment with irradiation. Note the absence of dying cells in *F*. Quantification is presented in Figure 4E.

mental Fig. 1B). Hence, as expected, the p53 enhancer governs stress-responsive induction at the *rpr* locus in vivo. Surprisingly, *hid* and *skl* were also unresponsive in $D2^{p53RE}$ animals (Fig. 1C,D), but induction of *hid* was unperturbed in $D3^{control}$ mutants and $D2^{p53RE}$ heterozygotes (Fig. 1C; Supplemental Fig. 1A). Unlike *rpr* and *hid*, induction of *skl* was affected in $D3^{control}$ mutants (Fig. 1D), possibly due to the proximity of the $D3^{control}$ breakpoint to *skl*. To determine whether other genes in the Reaper region were affected by the p53RE deletion, we compared wild-type and $D2^{p53RE}$ irradiated samples using microarray analysis. As seen in Supplemental Figure 2, most other genes in this region are not expressed, while others were modestly affected or not changed in the p53RE mutant. Together, these observations show that elimination of the p53RE selectively impacted stimulus-induced behavior throughout the Reaper interval. Thus, a defined enhancer region specifies coordinated regulation of at least three genes over distances that span at least ~330 kb.

The p53RE region contacts targets in cis

To regulate local RIPD genes, the p53 enhancer could physically contact these genes through chromosomal looping conformations (Baker 2011). To test this possibility, we analyzed genomic structure at the p53RE using 3C. This method combines cross-linking, ligation, and PCR to detect chromatin contact sites in vivo (Dekker et al. 2002). Throughout these studies, stringent controls ensured that only authentic contacts were detected (see the Supplemental Material). Furthermore, to improve our experimental resolution, we measured all 3C contacts using a droplet digital PCR (ddPCR) system (see the Supplemental Material; Hindson et al. 2011; Pinheiro et al. 2012), which enables direct quantitative comparisons among 3C contacts. In this d3C assay, labeled probes are used in multiplexed PCR reactions that are partitioned into thousands of droplets and titrated such that each droplet yields a binary output when read by a detector. Because reactions are cycled to saturation, the number of positive and negative droplets produce an absolute measurement of cross-linked starting molecules, enabling efficient comparisons across samples (see the Supplemental Material; Supplemental Figs. 3, 4; Pinheiro et al. 2012).

As seen in Figure 2B and Supplemental Figures 5 and 6, we discovered numerous contacts between the p53 enhancer and local targets in the Reaper region. For example, variable primers 2–4 indicate contacts near *hid*. We also considered the possibility that p53 might influence p53RE interactions with target sites. Therefore, we profiled 3C contacts in $p53^{-}$ animals using d3C (Supplemental Fig. 5). Overall, d3C contact patterns were similar, and differences observed in $p53^{-}$ embryos were not statistically significant. These data suggest that the p53 protein is not generally required for these chromatin contacts. To determine whether irradiation influences chromatin contacts, we also profiled d3C patters in irradiated embryos (Supplemental Fig. 6). We found few differences between control and irradiated embryos, suggesting that chromatin interactions are generally preconfigured rather than assembled after stress.

The p53RE restores contacts from an ectopic position

To determine whether the p53RE region is sufficient to establish *trans* looping contacts, we profiled contacts formed by an ectopic enhancer in animals that lacked the native enhancer. Specifically, we used a 19-kb rescue construct (BAC 17) (see the Supplemental Material) containing this enhancer on the second chromosome, which was crossed into the $D2^{p53RE}$ line to generate a strain referred to as 17; $D2^{p53RE}$. Some, but not all, looping contacts were restored to the Reaper region despite the fact that the p53RE was relocated to a nonnative site on a different chromosome (Fig. 2C,D). For example, contacts to region 7 are significantly above background, and regions near *rpr* and *skl* display interactions with the exogenous p53RE as well. To verify these *trans* contacts, we performed FISH on 17; $D2^{p53RE}$ animals (Fig. 2E–H). For these studies, we used a probe specific to the ectopic rescue fragment along with probes for either *hid* or *skl*. For negative controls, we quantified p53RE colocalization with the Bithorax region (BX-C). Automated software was used to authenticate colocalization events, enabling unbiased surveys of whole-mount embryos. As seen in Figure 2, E–H, and Supplemental Table 1, these studies verified that the ectopic p53RE fragment interacts with endogenous targets in a subset of cells. We also tested whether a smaller fragment, Rpr11, could restore contacts to targets in the Reaper region from an ectopic location in *trans*. Using d3C and FISH, we found that

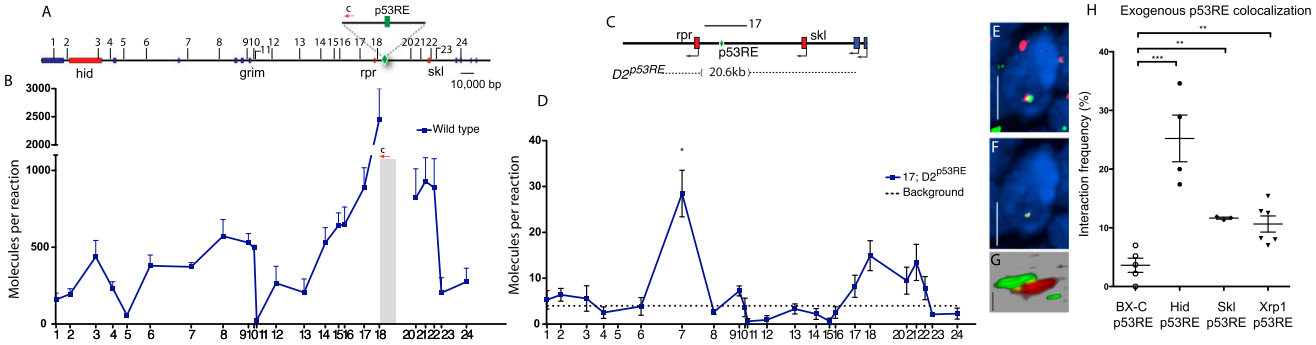

Figure 2. The p53 enhancer contacts multiple genes in the Reaper region from native and ectopic sites. (*A*) A schematic of the Reaper region illustrates radiation-inducible apoptotic genes (red) and nonrelevant genes (blue). Numbers label variable 3C primers designed at HindIII sites. A 3.7-kb HindIII fragment spanning the p53RE (green diamond) is magnified here to show the position of the constant (c) primer (red arrow) and the canonical p53-binding site (green rectangle). (*B*) Quantitative d3C reactions generated using the constant primer (c), CFPrev2 (red arrow in *A*), and variable primers indicated (numbers in *A*) in wild-type animals. Regions that contact the p53 enhancer produce 3C products quantified as starting molecules per reaction (see the Supplemental Material). Plots are averages of three independent experiments, and error bars represent the SEM. Not all HindIII sites are illustrated. (*C*) The p53RE (green diamond) and the $D2^{p53RE}$ deletion are shown along with a rescue BAC containing the p53RE within a 19.3-kb fragment (labeled as 17) inserted on the second chromosome and placed into the $D2^{p53RE}$ background (*17; $D2^{p53RE}$*). (*D*) Rescue animals shown in *C* were profiled for the indicated 3C contacts using CFPrev2 in the Reaper region. The native p53RE is missing in this rescue strain, and all products represent *trans* contacts between the ectopic p53RE and the indicated locus. Plots represent the average of three independent experiments. Error bars indicate the SEM. An asterisk represents contacts significantly different from background (two-tailed *t*-test, $P = 0.05$). (*E–G*) Confocal images of FISH between the ectopic p53RE (green) and endogenous *skl* (red) on *17; $D2^{p53RE}$* embryos (0–7 h). (*G*) The colocalized signal (yellow in *F*) in the confocal images is shown as an Imaris projection. Bars: *E,F*, 2 μm; *G*, 0.5 μm. (*H*) Quantification of colocalized signals in rescue transgenic (*17; $D2^{p53RE}$*) animals of the exogenous p53RE and endogenous *hid*, *skl*, or *xrp1*. Coincidence of the BX-C region and the ectopic p53RE is a negative control. The percentage represents the number of cells with overlapping signals out of the total cells containing both green and red signals for each confocal stack. (*) $P = 0.05$; (**) $P = 0.005$; (***) $P = 0.0005$; two-tailed *t*-test.

Rpr11 was able to contact sites at *hid* and *skl* (Supplemental Fig. 7). Hence, the p53RE region can assemble contacts with native target sites from ectopic positions in *trans*. Since only a subset of normal contacts was observed, constraints associated with ectopic positions might limit chromatin movements needed to produce full wild-type conformations. Alternatively, additional sequences not contained in the ectopic fragment may be needed to fully restore wild-type contact patterns.

Long-distance control by the p53RE

To determine whether the native p53RE normally governs distant target genes outside of the Reaper region, we examined a previously studied RIPD gene that is not linked to the p53RE and also does not reside near a computed p53-binding site (Akdemir et al. 2007). This gene, known as *xrp1*, ranks among the most acutely responsive RIPD genes and, like *rpr*, exhibits rapid induction within 15 min after radiation exposure (Brodsky et al. 2004). As seen in Figure 3A, *xrp1* regulation was unperturbed in $D3^{control}$ animals. However, this gene was strikingly unresponsive in $D2^{p53RE}$ homozygotes despite the fact that it resides across the centromere and >20 Mb from the p53RE.

The endogenous p53RE contacts long-distance targets

To determine how the p53RE regulates *xrp1*, we used d3C to examine whether the p53RE interacts with the *xrp1* locus. Figure 3 shows that this enhancer, which resides on the left arm of chromosome 3, interacts with the *xrp1* locus (Fig. 3G) on the right arm of chromosome 3. To independently corroborate these findings, we conducted FISH experiments using probes specific for the p53RE and *xrp1* (Fig. 3C–E). As a positive control, previously reported contacts in the BX-C region were visualized (see Supplemental Table 1; Lanzuolo et al. 2007), and, as a negative control, we included colocalization between the p53RE and *rp49*. As seen in Figure 3B, the in vivo frequency of contact between the p53 enhancer and *xrp1* ranged from 8% to 46%. Clearly, not all nuclei registered colocalization events, suggesting that the p53 enhancer makes physical contact to *trans* targets within only a subset of cells at any given time. Nevertheless, the frequencies seen for this *trans* contact are similar to reports for other enhancers and their long-range *cis* targets (Lomvardas et al. 2006).

To determine whether an ectopically positioned p53RE is also sufficient to establish looping contacts with *xrp1*, we profiled *17; $D2^{p53RE}$* animals using d3C assays. Like contacts seen in the Reaper region (Fig. 2D), we found that looping contacts near *xrp1* were also re-established despite the fact that the p53RE was relocated to a non-native site on a different chromosome (Fig. 3H). To verify these *trans* contacts, we performed FISH using rescued animals lacking the native enhancer. We used a probe specific to the ectopic rescue fragment along with a probe for *xrp1* and verified that a significant subset of cells contained contacts between the exogenous p53RE and *xrp1* (Fig. 2H). Hence, the p53RE can assemble appropriate contacts with long-distance target sites from ectopic positions in *trans* in a sequence-specific manner.

The p53RE restores regulation from an ectopic position

We also tested whether the p53 enhancer could direct stimulus-dependent regulation of target genes when relocated to ectopic positions. For these studies, *17; $D2^{p53RE}$* or *Rpr11; $D2^{p53RE}$* embryos were irradiated and assessed for induction of *rpr*, *skl*, *hid*, and *xrp1* using digital RT–PCR. As seen in Figure 4, stimulus-induced

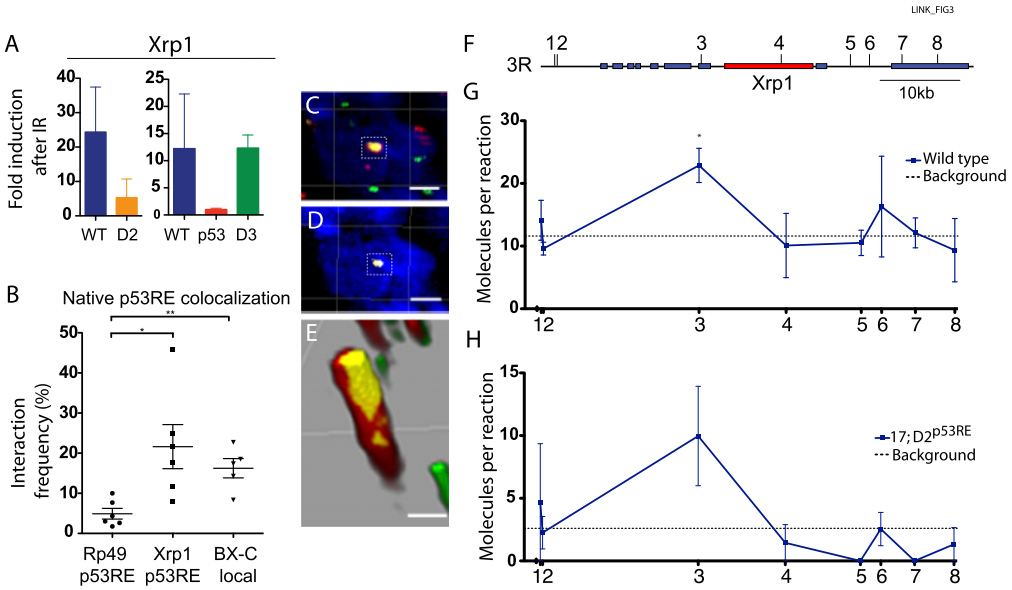

Figure 3. The p53 enhancer contacts distant regulated target genes from native and ectopic locations. (*A*) Quantitative RT–PCR was used to assess radiation-induced expression of the RIPD gene *xrp1* in wild-type, $D2^{p53RE}$, $D3^{control}$, and *p53* mutant embryos. *xrp1* is nonresponsive in $D2^{p53RE}$ animals, while stress-induced expression remains unchanged in $D3^{control}$. $p53^{-}$ animals are unresponsive. Plots show the average of three biological replicates with standard deviation. *rp49* expression was used for normalization. (*B*) Quantification of colocalized FISH signals (*C–E*) in wild-type animals. The percentage represents the number of cells with overlapping signals relative to the total cells containing both green and red signals for each confocal stack. Colocalizing probes within the BX-C region were included as a positive control, and *rp49* served as a negative control. (*) $P = 0.05$; (**) $P = 0.005$; two-tailed *t*-test. See Figure 2H for FISH colocalization between *xrp1* and the ectopic p53RE. (*C–E*) Representative FISH confocal images of the p53RE (green) and *xrp1* (red) in wild-type embryos (0–7 h). (*E*) The colocalized signal (yellow in *D*) boxed in the confocal images is shown as an Imaris projection. Bars, 1 μm. (*F*) A schematic of the *xrp1* locus on 3R illustrates the radiation-induced, p53-dependent sequence (red) and other genes (blue). Variable primers designed at HindIII sites are numbered accordingly. (*G*) Contacts between the p53RE (3L) and distant sites on 3R (*xrp1*) were profiled in d3C reactions using wild-type animals with the constant primer CFPrev2 (red arrow in Fig. 2A) and variable primers (see Supplemental Table 3). (*H*) *17; $D2^{p53RE}$* animals (see Fig. 2C) were profiled for the indicated 3C contacts using CFPrev2 in the *xrp1* region. In these animals, the native p53RE is missing, and all products represent *trans* contacts with the ectopic p53RE. Quantified 3C profiles are shown as an average of three independent trials, with error bars representing the SEM. An asterisk represents contacts significantly different from background (two-tailed *t*-test, $P = 0.05$).

transcript levels of these RIPD genes are strongly attenuated in $D2^{p53RE}$ embryos. However, in *17; $D2^{p53RE}$* animals containing the ectopic p53RE transgene, baseline and stimulus-responsive transcription of *hid* and *xrp1* was restored to wild-type levels (Fig. 4A,B), while *Rpr11; $D2^{p53RE}$* animals mildly rescued *hid* and *xrp1* transcription (Supplemental Fig. 7). Notably, radiation-responsive expression of local targets *rpr* and *skl* was not restored with either rescue transgene (Fig. 4C,D; Supplemental Fig. 7), perhaps reflecting the fact that these genes are normally adjacent to the p53RE (see Fig. 1). To ask whether partial restoration of RIPD gene expression affected cellular responses, we profiled irradiation-induced cell death in $D2^{p53RE}$ and *17; $D2^{p53RE}$* embryos. Figure 4E illustrates that stress-induced cell death was partially restored in *17; $D2^{p53RE}$* animals (Fig. 4E). Since neither *rpr* nor *skl* expression was rescued, both of these genes appear to be needed for robust embryonic irradiation-induced cell death. Hence, partial restoration of gene expression programs correlates with partial rescue of this phenotype.

The p53RE can generate simultaneous contacts with multiple targets in a single cell

To test whether multiple targets can simultaneously contact the p53RE in a single cell, we performed three-color FISH using probes for the p53RE, *hid*, and *xrp1* (Fig. 5). We found colocalization of all three loci within 23% of cells, indicating that the p53RE can contact multiple targets within a single nucleus.

Here we present in vivo functional evidence that a single enhancer region can specify regulation of multiple targets in *cis* and in *trans*. Using tailored deletions, we found that a p53 regulatory element controlled stimulus-dependent induction of multiple genes, with effects on targets that range from 4 kb to 330 kb throughout the *Drosophila* Reaper region. In our studies, the p53RE also regulated *xrp1*, a genetically unlinked target residing across the centromere. Furthermore, when transplanted to ectopic locations, contacts with target sites were re-established and regulation of some target genes was restored. Together, these functional studies offer compelling evidence that an enhancer transmits regulatory activity in *trans* through direct physical contact.

In principle, long-range regulation of *xrp1* by the native p53RE could involve local induction of an activator that subsequently induces distant genes, but this type of expression cascade would not explain the data presented here. First, no correlation exists between the timing of RIPD gene induction and proximity to the p53RE. Second, *cis* targets in the Reaper interval encode products with no known function in the nucleus or in transcription (Tweedie et al. 2009). Third, conventional expression cas-

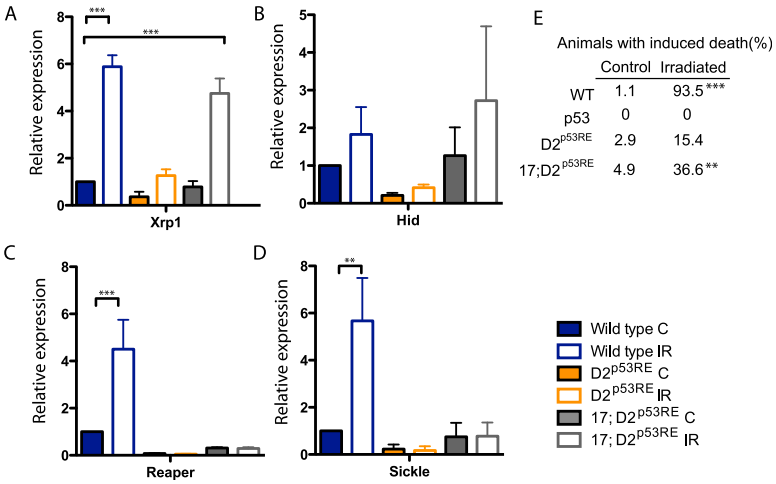

Figure 4. The p53 enhancer partially restores regulation from ectopic sites in *trans*. Embryos homozygous for the $D2^{p53RE}$ deletion with (*17; $D2^{p53RE}$*) or without the rescue fragment (see Fig. 2C) were irradiated and tested for regulation of p53 target genes using digital RT–PCR (3-h recovery). Results in *A–D* are plotted as expression relative to unirradiated wild-type samples isolated in parallel. *xrp1* (*A*), *hid* (*B*), *rpr* (*C*), and *skl* (*D*) transcripts were assayed as indicated by the color code (*bottom right*). (*E*) The rescue strain (*17; $D2^{p53RE}$*) was tested for damage-induced apoptosis in early embryos as in Figure 1, E and F. The data in *E* show the percentage of animals that have induced cell death for each genotype with (*right*) or without (*left*) irradiation. Note that animals carrying the rescue transgene (*17; $D2^{p53RE}$*) partially rescued apoptotic phenotypes in this assay. Significance was determined by one-way ANOVA with multiple comparisons post-test; (**) P = 0.01; (***) P = 0.001) in all panels.

cades would not account for the restoration of regulation and contacts by a transgenic rescue fragment. Therefore, we favor the idea that long-range regulation by the p53RE involves chromosomal architectures that link this enhancer to target genes regardless of whether they are in *cis* or in *trans*.

Using either 3C or direct visualization (Spilianakis et al. 2005; Lomvardas et al. 2006), suggestive chromatin links between enhancers and distant genomic sites in *trans* have been reported (Celniker et al. 2009; Tanizawa et al. 2010; The ENCODE Project Consortium 2011). Few have been genetically tested (Williams et al. 2010), and, where functionally studied, detectable effects were not seen (Fuss et al. 2007). Our finding that productive looping contacts can be assembled from a foreign site suggests that determinants of long-range chromatin interactions are modular and probably specified through sequence motifs, secondary structures, and epigenetic features that occur in vivo. We further note that the presence of contacts is not sufficient for target induction. For example, despite loops between the native p53RE and sites near *grim* or contacts between the ectopic p53RE and sites near *rpr* and *skl*, transcriptional induction was not seen (Fig. 4; Supplemental Figs. 1C, 7). Therefore, elements that map outside of the rescue fragment or constraints imposed by flanking chromatin may also be important.

Given that p53 enhancers in both flies and humans share a common sequence motif (Brodsky et al. 2000), mechanisms by which these response elements form long-range interactions in *trans* may be conserved. It will be interesting to see whether other enhancer regions share this property (Bulger and Groudine 2011). Likewise, it will be important to determine whether these contacts are mediated through complexes involving proteins such as Cohesin, Mediator (Kagey et al. 2010; Phillips-Cremins et al. 2013), Ldb1 (Deng et al. 2012), Polycomb (Bantignies et al. 2011), or CTCF (Williams and Flavell 2008). If broadly generalized, the precedent established here could offer a framework that helps explain genetic disease alleles mapping to noncoding sequences (Velagaleti et al. 2005; Visel et al. 2009).

Materials and methods

RT–PCR

Embryos were collected for 2.5 h, aged for 2.5 h, either mock-treated or irradiated at 40 Gy followed by a 1.5-h (Figs. 1, 3) or 3-h (Fig. 4) recovery, and treated as in the Supplemental Material.

Acridine orange

Embryos were collected for 2 h, aged for 2.5 h, and either mock-treated or irradiated at 40 Gy and stained as in Abrams et al. (1993).

3C

Four-hour to 6.5-h embryos were dechorionated with 50% bleach and fixed at the interface of equal amounts of heptane and 2% formaldehyde in the presence of 50 mM HEPES (pH 7.6), 100 mM NaCl, 0.1 mM EDTA, and 0.5 mM EGTA while shaking for 15 min. Embryos were treated as in the Supplemental Material and Miele et al. (2006) and Hagege et al. (2007) using HindIII as the restriction enzyme of choice.

FISH

BACs containing fragments of interest (see Supplemental Table 2) were labeled with Invitrogen's FISH Tag DNA Multicolor kit and purified as suggested. Embryos were fixed in 4% formaldehyde in PBS and hybridized as described in *Drosophila* protocols (Sullivan et al. 2000).

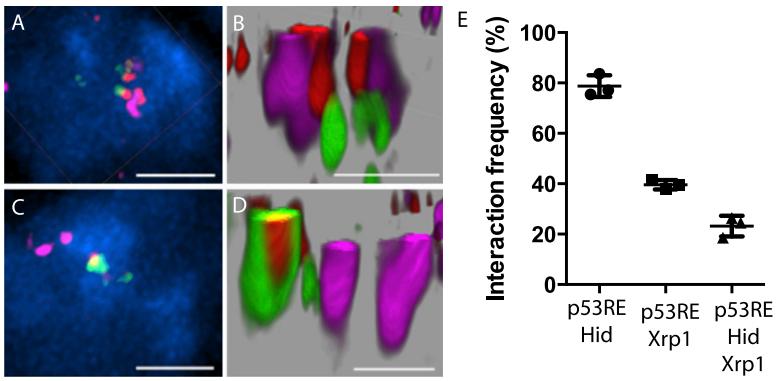

Figure 5. The p53 enhancer region can contact multiple targets in a single nucleus. Confocal images (*A,C*) and Imaris projections (*B,D*) of three-color FISH in *Drosophila* embryos. (*A,B*) Examples of three-way colocalization for the p53RE (green), *hid* (red), and *xrp1* (purple) probes. (*C,D*) Examples in which only the p53RE and *hid* colocalize. Bars, 2 μm. (*E*) Quantification of colocalization as indicated. Note that only nuclei containing signals for all three probes were counted.

Acknowledgments

We thank Erin Regan, Ashley Olivo, and Shino Murakami for technical assistance; Abhijit Budge and Kate Luby-Phelps with the University of Texas Southwestern Live-Cell Imaging Facility for assistance with imaging; and Bill Nordstrom, Wan-Jin Lu, and Alex D'Brot for discussion. This work was supported by grants to J.M.A. from the Cancer Prevention Research Institute of Texas (RP110076), the National Institute of General Medical Sciences (R01GM072124), the National Institute on Alcohol Abuse and Alcoholism (R01AA017328), the Welch foundation (I-1727), and the Ellison Medical Foundation. N.L. and P.K. were supported by National Research Service Awards (F31NS058118 and F31GM108472). M.O. and G.G.-H. contributed to unshown data. P.K. conducted three-way FISH, and N.L. conducted all other experiments. N.L. and J.M.A. designed the study, analyzed the data, and wrote the manuscript.

References

Abrams JM, White K, Fessler L, Steller H. 1993. Programmed cell death during *Drosophila* embryogenesis. *Development* **117:** 29–44.

Akdemir F, Christich A, Sogame N, Chapo J, Abrams JM. 2007. p53 directs focused genomic responses in *Drosophila*. *Oncogene* **26:** 5184–5193.

Baker M. 2011. Genomics: Genomes in three dimensions. *Nature* **470:** 289–294.

Bantignies F, Roure V, Comet I, Leblanc B, Schuettengruber B, Bonnet J, Tixier V, Mas A, Cavalli G. 2011. Polycomb-dependent regulatory contacts between distant hox loci in *Drosophila*. *Cell* **144:** 214–226.

Brodsky MH, Nordstrom W, Tsang G, Kwan E, Rubin GM, Abrams JM. 2000. *Drosophila* p53 binds a damage response element at the reaper locus. *Cell* **101:** 103–113.

Brodsky MH, Weinert BT, Tsang G, Rong YS, McGinnis NM, Golic KG, Rio DC, Rubin GM. 2004. *Drosophila melanogaster* MNK/Chk2 and p53 regulate multiple DNA repair and apoptotic pathways following DNA damage. *Mol Cell Biol* **24:** 1219–1231.

Bulger M, Groudine M. 2011. Functional and mechanistic diversity of distal transcription enhancers. *Cell* **144:** 327–339.

Celniker SE, Dillon LA, Gerstein MB, Gunsalus KC, Henikoff S, Karpen GH, Kellis M, Lai EC, Lieb JD, MacAlpine DM, et al. 2009. Unlocking the secrets of the genome. *Nature* **459:** 927–930.

Dekker J, Rippe K, Dekker M, Kleckner N. 2002. Capturing chromosome conformation. *Science* **295:** 1306–1311.

Deng W, Lee J, Wang H, Miller J, Reik A, Gregory PD, Dean A, Blobel GA. 2012. Controlling long-range genomic interactions at a native locus by targeted tethering of a looping factor. *Cell* **149:** 1233–1244.

The ENCODE Project Consortium. 2011. A user's guide to the encyclopedia of DNA elements (ENCODE). *PLoS Biol* **9:** e1001046.

Freed-Pastor WA, Prives C. 2012. Mutant p53: One name, many proteins. *Genes Dev* **26:** 1268–1286.

Fuss SH, Omura M, Mombaerts P. 2007. Local and *cis* effects of the H element on expression of odorant receptor genes in mouse. *Cell* **130:** 373–384.

Hagege H, Klous P, Braem C, Splinter E, Dekker J, Cathala G, de Laat W, Forne T. 2007. Quantitative analysis of chromosome conformation capture assays (3C-qPCR). *Nat Protoc* **2:** 1722–1733.

Hindson BJ, Ness KD, Masquelier DA, Belgrader P, Heredia NJ, Makarewicz AJ, Bright IJ, Lucero MY, Hiddessen AL, Legler TC, et al. 2011. High-throughput droplet digital PCR system for absolute quantitation of DNA copy number. *Anal Chem* **83:** 8604–8610.

Kagey MH, Newman JJ, Bilodeau S, Zhan Y, Orlando DA, van Berkum NL, Ebmeier CC, Goossens J, Rahl PB, Levine SS, et al. 2010. Mediator and cohesin connect gene expression and chromatin architecture. *Nature* **467:** 430–435.

Lanzuolo C, Roure V, Dekker J, Bantignies F, Orlando V. 2007. Polycomb response elements mediate the formation of chromosome higher-order structures in the bithorax complex. *Nat Cell Biol* **9:** 1167–1174.

Lomvardas S, Barnea G, Pisapia DJ, Mendelsohn M, Kirkland J, Axel R. 2006. Interchromosomal interactions and olfactory receptor choice. *Cell* **126:** 403–413.

Lu WJ, Amatruda JF, Abrams JM. 2009. p53 ancestry: Gazing through an evolutionary lens. *Nat Rev Cancer* **9:** 758–762.

Menendez D, Inga A, Resnick MA. 2009. The expanding universe of p53 targets. *Nat Rev Cancer* **9:** 724–737.

Miele A, Gheldof N, Tabuchi TM, Dostie J, Dekker J. 2006. Mapping chromatin interactions by chromosome conformation capture. *Curr Protoc Mol Biol* **74:** 21.11.1–21.11.20.

Ollmann M, Young LM, Di Como CJ, Karim F, Belvin M, Robertson S, Whittaker K, Demsky M, Fisher WW, Buchman A, et al. 2000. *Drosophila* p53 is a structural and functional homolog of the tumor suppressor p53. *Cell* **101:** 91–101.

Phillips-Cremins JE, Sauria ME, Sanyal A, Gerasimova TI, Lajoie BR, Bell JS, Ong CT, Hookway TA, Guo C, Sun Y, et al. 2013. Architectural protein subclasses shape 3D organization of genomes during lineage commitment. *Cell* **153:** 1281–1295.

Pinheiro LB, Coleman VA, Hindson CM, Herrmann J, Hindson BJ, Bhat S, Emslie KR. 2012. Evaluation of a droplet digital polymerase chain reaction format for DNA copy number quantification. *Anal Chem* **84:** 1003–1011.

Sogame N, Kim M, Abrams JM. 2003. *Drosophila* p53 preserves genomic stability by regulating cell death. *Proc Natl Acad Sci* **100:** 4696–4701.

Spilianakis CG, Lalioti MD, Town T, Lee GR, Flavell RA. 2005. Interchromosomal associations between alternatively expressed loci. *Nature* **435:** 637–645.

Sullivan W, Ashburner M, Hawley R. 2000. Drosophila *protocols*. Cold Spring Harbor Laboratory Press, Cold Spring Harbor, NY.

Tanizawa H, Iwasaki O, Tanaka A, Capizzi JR, Wickramasinghe P, Lee M, Fu Z, Noma K. 2010. Mapping of long-range associations throughout the fission yeast genome reveals global genome organization linked to transcriptional regulation. *Nucleic Acids Res* **38:** 8164–8177.

Tweedie S, Ashburner M, Falls K, Leyland P, McQuilton P, Marygold S, Millburn G, Osumi-Sutherland D, Schroeder A, Seal R, et al. 2009. FlyBase: Enhancing *Drosophila* gene ontology annotations. *Nucleic Acids Res* **37:** D555–D559.

Velagaleti GV, Bien-Willner GA, Northup JK, Lockhart LH, Hawkins JC, Jalal SM, Withers M, Lupski JR, Stankiewicz P. 2005. Position effects due to chromosome breakpoints that map approximately 900 kb upstream and approximately 1.3 Mb downstream of SOX9 in two patients with campomelic dysplasia. *Am J Hum Genet* **76:** 652–662.

Visel A, Rubin EM, Pennacchio LA. 2009. Genomic views of distant-acting enhancers. *Nature* **461:** 199–205.

Vousden KH, Prives C. 2009. Blinded by the light: The growing complexity of p53. *Cell* **137:** 413–431.

Williams A, Flavell RA. 2008. The role of CTCF in regulating nuclear organization. *J Exp Med* **205:** 747–750.

Williams A, Spilianakis CG, Flavell RA. 2010. Interchromosomal association and gene regulation in trans. *Trends Genet* **26:** 188–197.